UV Assisted Enhanced Photodegradation of Carbaryl Pesticide with Ag Doped ZnO NPs

A. Satheesh[1*], J. C. Rao[2], M. V. V. Ramanjaneyulu[3], K. N. Jogayya[4], K. V. Kalyan[5], A. Kumar[6], H. Usha[7]

[1]Department of Chemistry, Centurion University of Technology and Management, Vizianagram (Andhra Pradesh), India

[2]Department of Physics, Govt. Degree College, Rajam(Andhra Pradesh), India

[3]Department of Chemistry, KGRL (A) College, Bhimavaram, West Godavari (Andhra Pradesh), India

[4]School of Forensic Science, Centurion University of Technology and Management, Jatni (Odisha), India

[5]School of Paramedical and Allied health sciences, Centurion University of Technology and Management, Vizianagram (Andhra Pradesh), India

[6]Department of Management studies, Centurion University of Technology and Management, Vizianagram (Andhra Pradesh), India

[7]Department of Chemistry, Govt. Polytechnic for Women, Srikakulam (Andhra Pradesh), India

Abstract

Every year approximately one million tonnes of pesticide effluents are releasing into natural streams and water bodies from nearby industries and agricultural fields. It is necessary to remove pesticides and their residues from water bodies to protect environment and ecosystem. Photodegradation is an effective method to remove the organic contaminants from water bodies due to its low cost, environmental friendliness and absence of secondary pollutants. This work presents about the synthesis, characterization of pure and silver doped ZnO nanoparticles (NPs) and their efficiency towards the photo degradation of carbaryl pesticide. Pure and Ag doped nanoZnO particles were synthesized by wet chemical method using zinc nitrate as precursor and the synthesized nano particles were studied using FT-IR, XRD, UV-Vis, SEM, EDAX, TEM and fluorescence spectral analysis to evaluate its structural, morphological, optical and fluorescent properties. Carbaryl pesticide was taken at a fixed concentration of 5 ppm, and subjected to photo degradation by adding 5 mg/L of pure and Ag doped nanoZnO separately under UV irradiation. It is observed that in 60 min 90 % of the pesticide was degraded with pure ZnO NPs and 98 % with Ag doped ZnO NPs.

Corresponding author: satheeshampolu@gmail.com

1. Introduction

Pesticides are chemicals that are used to eradicate undesirable organisms from agricultural land, and private gardens. Pesticides may contaminate water bodies, soil, turf, and vegetation in addition to killing weeds and bugs. Pesticides are also harmful to a wide range of other organisms including fish, birds, non-target plants, and beneficial insects. Exposure to pesticides can cause a variety of health troubles like blisters, stinging eyes, blindness, rashes, diarrhea, dizziness, nausea, and chronic diseases like immune toxicity, developmental and neurological toxicity, reproductive harm, birth defects, cancer, and disruption of the endocrine system [1-6]. Raising the application of more quantities of pesticides is a major concern for the groundwater, surface water, coastal, and Marine habitats. Pesticides in water resources have been considered likely mutagens since they contain elements that might cause DNA variations, which leads to great damage to living organisms and ecosystems. As per the statistical data of the World Health Organization every year nearly one million people face acute poisoning by pesticide contact, a death rate of 0.4-1.9 % is recorded [7,8].

Carbaryls are a category of insecticide, similar to organophosphate insecticides (OP) in terms of structure and mechanism. It has been approved for use in pesticides since 1959. Carbaryl is the common name for the active ingredient, 1-naphthyl-N-methylcarbamate is an off-white sold available in the market under many trade names (Fig. 1). In addition to many other outdoor pests, it is frequently used to manage ticks, aphids, fire ants, spiders, fleas, and other pests and is also used in some gardens to thin out blossoms on fruit trees in some gardens. Carbaryl is a cholinesterase inhibitor and hazardous to humans. The United States Environmental Protection Agency (EPA) has classed it as a probable human carcinogen. Contact can irritate the skin and eyes, resulting in a rash or burning sensation. Exposure may cause poisoning with blurred vision, nausea, sweating, vomiting, and abdominal pain. Carbaryl may cause headaches, weakness, and breathing problems and also affect the nervous system, kidneys, reproductive problems, and cancer [9-14]. In this connection, it is very essential to develop new technologies that promote the effective degradation of such bio-recalcitrant compounds. Recently photo catalysis has attracted a lot of interest because of its low cost, environmental friendliness, and lack of secondary pollutants in the process of degradation of pesticides, organic pollutants, textile dyes, and industrial wastage. The use of advanced oxidation processes (AOPs) is a successful method to accomplish the mineralization of these types of compounds is a promising method. These AOPs are distinguished by the production of highly reactive, oxidizing free radicals in aqueous solutions that exhibit significant oxidative potential. Heterogeneous photo catalysis is one of the successful methods suggested as AOP for eradicating organic contaminants in water. [15-18].
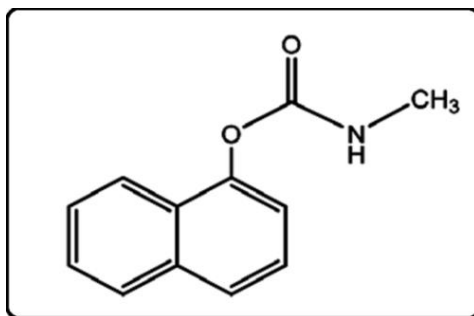
Fig. 1. Structure of carbaryl pesticide.

In recent years hybrid nano particles have drawn a lot of attention in the field of nano technology due to changing the properties of individual particles along with providing new and enhanced functionality. Semiconductor nano materials are intensively studied to remove organic pollutant molecules from water bodies. Zinc oxide is a semiconductor that is attracting a lot of attention because of its eco-friendliness, abundance, and absence of toxic components. It has been employed in numerous products because of its enticing properties such as photo catalysis, manufacturing of solar cells, sensors, electrical devices, and optical coatings [19-24]. Individually nanoZnO ensures weak optical properties and affinity to have point defects such as oxygen vacancy. Hence, in industries ZnO cannot be used directly. Therefore, it is necessary to dope ZnO with a noble metal to enhance its efficiency [25]. The purpose of this research work is to develop feasible and economical photo catalytic nano particles as well as an effective degradation method to remove carbaryl pesticide quickly from water, here we have reported the synthesis, characterization of pure and Ag doped ZnO nanoparticles (NPs) and their efficiency towards the photo degradation of carbaryl pesticide under Ultra Violet irradiation.

2. Experimental

2.1. *Materials and methods*

All the chemicals utilized in this work are of Analytical-grade and utilized directly without any additional purification. Zinc nitrate, silver nitrate and sodium hydroxide were acquired from Sigma Aldrich, USA and throughout the experiment doubly distilled water was utilized whenever required. All the reactions were conducted in an ambient condition at room temperature.

2.2. *Procedure for the synthesis of nanoZnO*

0.2 M solution of zinc nitrate hexahydrate ($Zn(NO_3)_2 \cdot 6H_2O$) was taken in 500 mL of beaker and added 0.4 M sodium hydroxide (NaOH) drop-wise by stirring continuously at room temperature to form metal hydroxides. The stirring procedure was continued at 85°C

for 6 h to obtain as-synthesized powder. Thus, the as-synthesized powder was calcinedin Muffle furnace at 600 $^{\circ}$C for 2 h and then the furnace was cooled. The resulting product was characterized by XRD, SEM and EDAX [26].

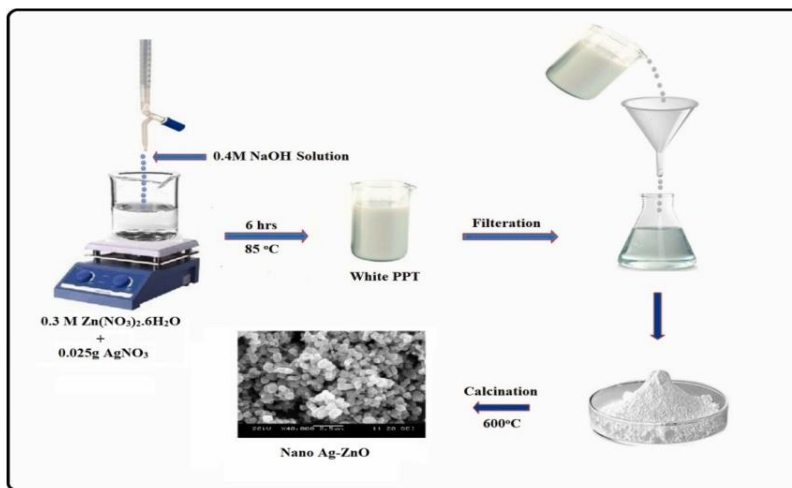

Fig. 2. Schematic diagram of synthesis of Ag doped nanoZnO.

2.3. *Procedure for the Synthesis of Ag doped nanoZnO*

0.3 M solution of $Zn(NO_3)_2.6H_2O$ was taken in 500 mL of beaker, added 0.025 g of silver nitrate ($AgNO_3$) with continuous stirring for 30 min and 0.4 M NaOH was added drop-wise by stirring continuously at room temperature to form metal hydroxides. The stirring was continued at 85 $^{\circ}$C for 6 h to obtain as-synthesized powder. Thus, the as-synthesized powder was calcined in a Muffle furnace at 600 $^{\circ}$C for 2 h and then the furnace was cooled (Fig. 2). The resulting product was characterized by XRD, SEM and EDAX [27-30].

2.4. *Photocatalytic degradation studies*

In the current study, the photo degradation of carbaryl pesticide has been studied in aqueous dispersion under Ultra Violet irradiation using both pure and Ag doped nanoZnO as catalysts separately. The photo catalysis results show that the degradation efficiency of nanoZnO increased after doping with Ag. Two stock solutions of 250 mL, 5 ppm concentration were prepared, and transferred into the reactors. 5 mg of each nanoZnO and Ag doped ZnO was added respectively as photocatalyst. The suspension was initially stirred for 30 min under a completely dark environment to achieve the maximum adsorption. A stirring rate of 500 rpm was continued for the entire experiment. Later, the solution was introduced to a UV chamber for UV irradiation with vigorous stirring for a

fixed time. Within 60 min of the test solution being exposed to radiation, it was discovered that its color had changed from a light blue to a clear, colorless liquid. The degradation efficiency of carbaryl was determined by the UV-VIS spectrophotometer. To measure the concentration of pesticide solution after being exposed to UV irradiation for each 10 min, approximately 5 mL of the test solution was taken out and centrifuged to remove the catalyst particles from the suspension. Using the provided formula, the percentage of degradation was determined.

% of degradation = $\frac{Co-C}{Co}$ X 100

Where, C_o is the initial concentration of the test solution and C is the concentration of the solution after photocatalytic degradation.

2.5. *General mechanism involved in photodegradation*

Photo catalysis is the acceleration of a sequence of chemical events in the presence of light. Photocatalysis is a cutting-edge oxidation technique that heavily relies on hydroxyl radicals to break down organic molecules in water. When a photocatalyst is exposed to a photon with energy exceeding its band gap, the photocatalytic reaction is triggered instantly. When electrons in the valence band become excited and transfer to the conduction band, an electron-hole pair is created. Oxygen molecules later follow the electron in the photocatalyst's conduction band to form superoxide ions. Organic contaminants decay due to a continuous assault by hydroxyl radicals and superoxide ions. The photocatalytic degradation method is more significant than other degrading approaches due to its effectiveness, lack of sludge, and ability to environmentally remove organic contaminants from water. This approach utilises semiconductor materials to generate charge carriers in the presence of light, initiating chemical reactions like the oxidation of heavy metals, redox modification of organic pollutants, and reduction of carbon monoxide [34-40].
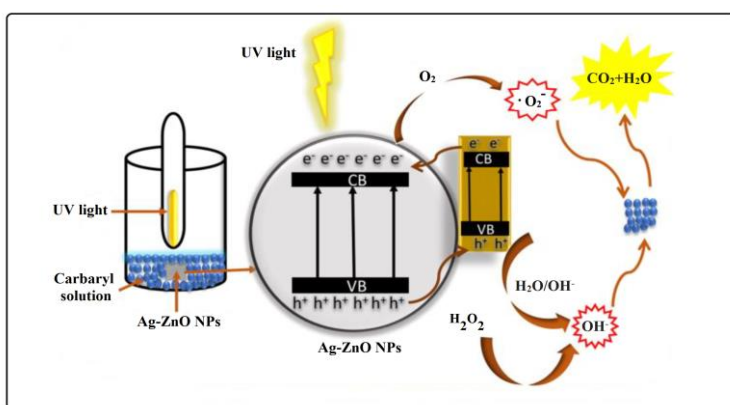

Fig. 3. Cartoon diagram for the photodegradation of Carbaryl pesticide.

2.6. *Characterizations*

FTIR (Fourier Transmission Infra-Red) spectroscopy (Perkin Elmer- Spectrum RX-IFTIR) was employed to identify the functional groups present in the synthesized product. The X-Ray diffraction patterns were recorded on Bruker X-Ray Diffractometer using graphite filtered CuK radiation ($\lambda = 1.54$ A°) at 40 KV with scanning rate of 30°/min (from $2\theta = 20\text{-}80°$). Morphology and size of the particles were determined by the 200 KeV Transmission Electron Microscope (TECNAI 200 Kv TEM-Fei, Electron Optics). Elemental composition of particles was determined by using SEM-EDAX (JEOL JSM 5600, EDS Model: INCA Oxford).

3. Results and Discussion

3.1. *FT-IR spectral analysis*

Fig. 4 shows the FTIR spectra of pure and Ag doped ZnO. The FTIR spectrum for Ag doped ZnO is similar to that of pure ZnO. FT-IR analysis was done using optimized parameters to determine the bond structure and related functional groups of the synthesized ZnO NPs. The band located at 450 cm^{-1} is attributed to the Zn–O stretching mode of the ZnO lattice. In these limits no further peak appears due to the doping silver, probably it was arises from homogeneous dispersion of Ag particles on the surface of ZnO without any cluster formation. The band that observed near 3400 cm^{-1}is assigned to vibration mode of O-H group. A weak band observed near 2900 cm^{-1} is assignable to C-H modes. The sharp band observed near 1400-1600 cm^{-1} iscorresponded to stretching vibration modes for C=O groups [26].

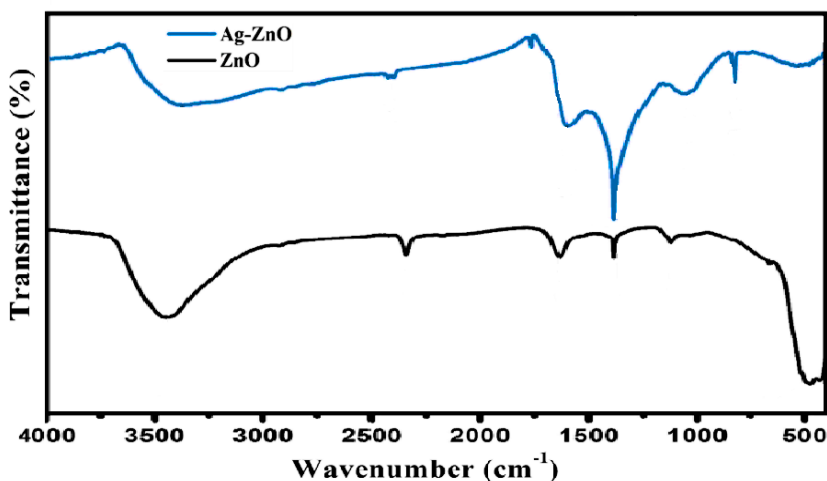Fig. 4. FT-IR spectrum of pure nanoZnO and Ag doped nanoZnO.

3.2. *X-Ray diffraction (XRD)*

Fig. 5 shows the XRD patterns of pure and Ag doped ZnO NPs. The diffraction pattern of Ag-ZnO NPs is almost similar to that of pure ZnO, which gives idea about crystallinity and size of the particles. The peaks at 31.80°, 34.47°, 36.29°, 47.58°, 56.62°, 62.90°, 66.40°, 67.98°, 69.11°, and 76.99°, determines the reflecting planes at (100), (002), (101), (102), (200), (112), (103), (110), (201), and (202) respectively. All the diffraction patterns shows the strong resemblance with the reported JCPDS (Joint Committee on Powder Diffraction Standards) belonging to hexagonal wurtzite crystal phase of synthesized particles [31].
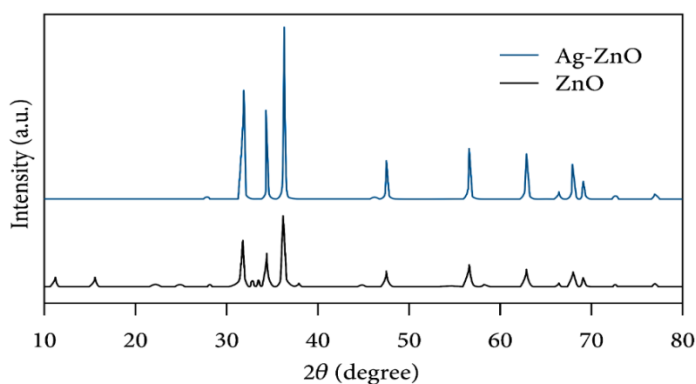

Fig. 5. XRD pattern of pure nanoZnO and Ag doped nanoZnO.

3.3. *SEM image analysis*

Figs. 6(a,b) and 6(c, d) show the SEM images of the synthesized pure and Ag-ZnO NPs respectively. From SEM images it is clear that the morphology of ZnO NPs has changed after doping with Ag. The SEM images determines that the synthesized Ag-ZnO NPs are well agglomerated with different sizes present in hexagonal shape. However, at higher magnification, it shows the cubic structure, that indicates the presence of Ag NPs and also showedhigh porosity, that represents that Ag NPs were coated on ZnO surface [31,32]. After doping with Ag the size of nanoZnO particles is almost doubled.
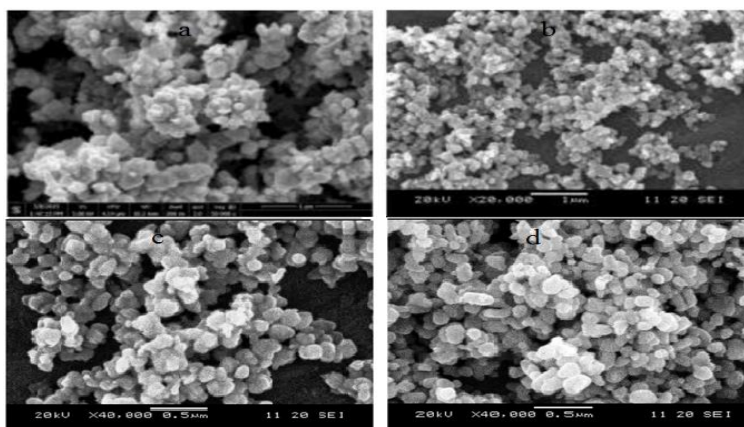
Fig. 6. SEM images of pure nanoZnO (a,b) and Ag doped nanoZnO (c,d).

3.4. *TEM) image analysis*

The samples of synthesized NPs were systematically analyzed by TEM to notify the morphology and actual size of the particles. The TEM image of nanoZnO (Fig. 7(a,b)) shows the presence of hexagonal wurtzite accumulated with a dimension of ~50 nm, the existing size of the NPs is found to be around 30 nm. Fig. 7(c,d) shows that the size of the Ag-ZnO NPs are in the range of 30–110 nm, the existing average size of the NPs is around 70 nm.
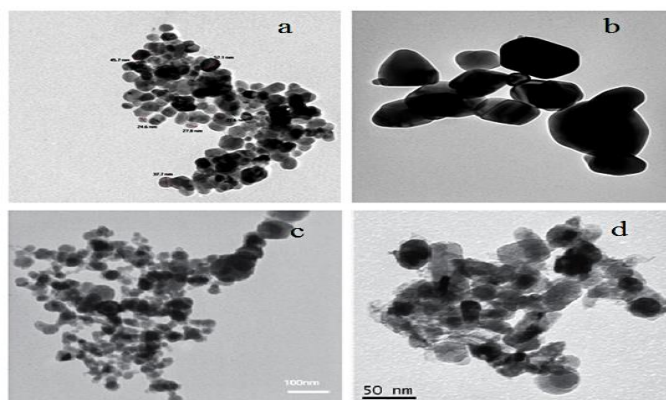

Fig. 7. TEM images of pure nanoZnO (a,b) and Ag doped nanoZnO (c,d).

3.5. *Energy Dispersive X-Ray (EDX) analysis*

The elemental composition of the synthesized NPs was confirmed by EDX analysis. Figs. 8a and 8b show the EDX spectra of pure and Ag doped ZnO NPs, indicate the presence of Zn, Ag and O with no other impurities [33].
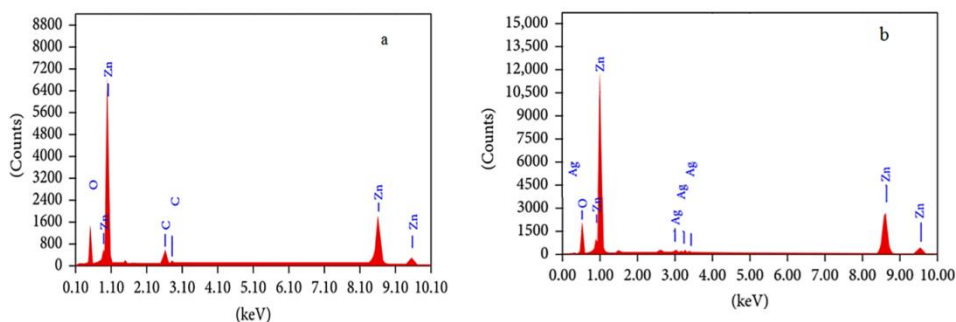
Fig. 8. EDX spectra of PurenanoZnO (a) and Ag doped nanoZnO (b).

3.6. *BET surface area analysis*

The specific surface area and porosity of Ag doped ZnO NPs were measured using nitrogen adsorption using a Micromeritics TRIstar 3020 nitrogen absorption equipment (USA). Fig. 9 shows the matching BET surface area and nitrogen adsorption–desorption isotherms of Ag doped ZnO NPs. Compared to pure ZnO NPs, the surface morphology of Ag/ZnO NPs revealed a significant and extensive region of porosity. The higly nanoporous structure of Ag/ZnO NPs produced significant increase in surface area, reaching 154.45 m^2/g from that of 75.68 m^2/g for pure ZnO NPs.
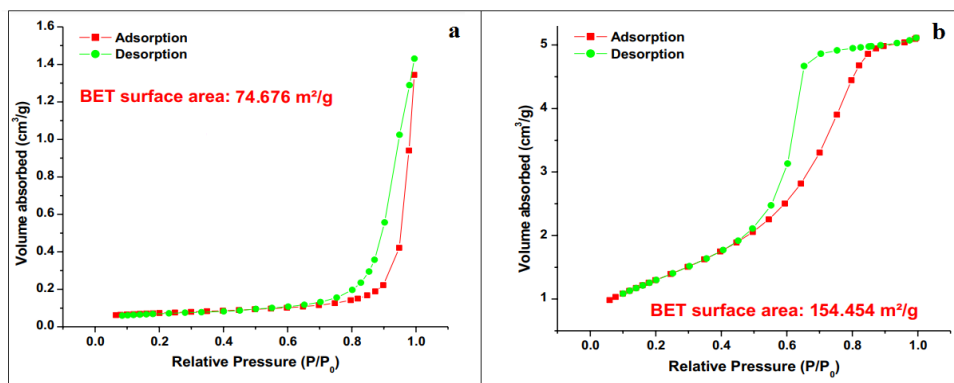

Fig. 9. BET surface area of pure ZnO (a) and Ag/ZnO (b) NPs.

3.7. *UV-Visible spectra*

Fig. 10 shows the UV-Visible spectra of pure nanoZnO and Ag doped nanoZnO which determines the light-absorbing capacity of the synthesized particles. The UV-Visible spectra of pure nanoZnO and Ag doped nanoZnO exhibits band gap absorption peaks at 364 nm and 366 nm respectively. It shows the peak has undergone Bathochromic shifting (red shifting) for doped NPs, that can be expressed by quantum size effects [37,40]. This

effect may be seen in SEM photos, where the diameter of the NPs increased with Ag doping.
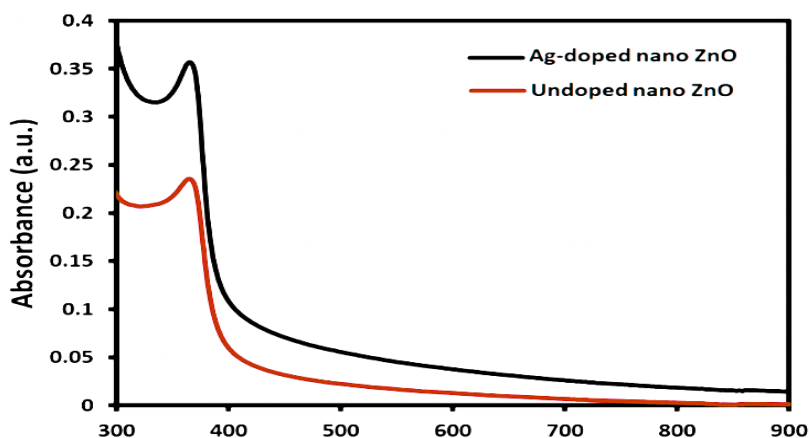

Fig. 10. UV-Visible spectra of pure nanoZnO and Ag doped nanoZnO.

3.8. *Chemical oxygen demand (COD) analysis*

The COD analysis typically provides a measure of the organic strength of industrial effluents. This analysis can estimate the total amount of oxygen required for the oxidation of organic compounds into carbon dioxide and water. Before and after degradation, the COD of the pesticide solution was calculated. The initial and final COD values of the carbaryl pesticide were determined. The drop in COD values proved the disappearance of color as well as break downof pesticide molecules. It is found that 11614 mg/L and 162 mg/L are the initial and final COD values for pure nanoZnO and 11614 mg/L and 134 mg/L for Ag doped nanoZnO respectively. Hence, it is clear that the degradation efficiency of nanoZnO is increased after doping with Ag.

3.9. *Total organic carbon (TOC) analysis*

TOC estimation is frequently employed to estimate the amount of organic carbon present in industrial effluent streams. Because it may be used to evaluate cutting-edge oxidation processes like photocatalysis, which was developed to decompose various inorganic and organic pollutants. Using nanoZnO, almost 90 % of the organic carbon was removed from the carbaryl pesticide solution in sixty min, but incase of Ag doped nanoZnO it is almost 98 %. This analysis again shows that Ag doped nanoZnO works well as a photocatalyst to degrade pesticide contaminants.

3.10. *Absorption spectral analysis*

The photocatalytic degradation reaction was carried out separately employing pure nanoZnO and Ag doped nanoZnO under UV irradiation. In order to track the degradation of carbaryl pesticide, the absorption spectra are periodically monitored. The photodegradation procedure is now more effective because it was possible to ascertain from this measurement how well the pesticide molecule relates to the nanoparticles. Fig. 11 exhibits the outcomes. In the presence of Ag doped nanoZnO, the highest absorption peak for the pesticide pollutant at 215 nm has been reduced at an astounding pace and has nearly vanished after 30 min of light illumination.
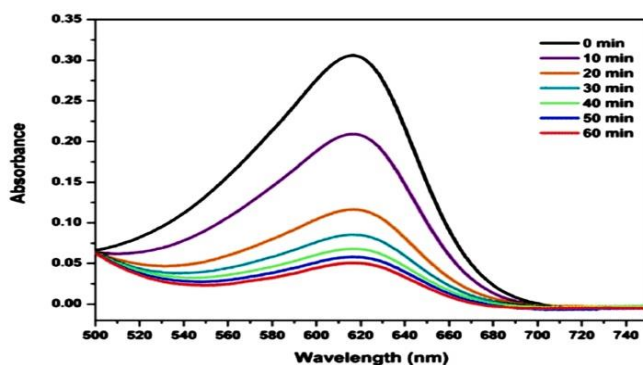

Fig. 11. UV-Visible absorption spectra for the degradation of carbaryl pesticide at different time intervals.

3.11. *Recycling of catalyst*

The cost of application and the stability of the photocatalyst are both important in terms of recycling capacity. The selected NPs were removed from the test solution by centrifugation after the degrading process was finished in order to examine the efficiency of NPs as photocatalyst in recycling. The recovered NPs were cleaned in double-distilled water, filtered, dried, and used in the subsequent carbaryl pesticide degradation cycle. This process was repeated for additional cycles, and the data presented in Table 1 shows pretty good degrading efficiency of carbaryl for five cycles. This has obviously specified the good recycling efficiency of the prepared NPs.

Table 1. Photo degradation of carbaryl pesticide efficiency of Ag doped nanoZnO.

Run no.	Degradation efficiency (%)
1	98
2	95
3	93
4	91
5	90

4. Conclusion

Pure and Ag doped nanoZnO particles were synthesized by wet chemical process and the characterization results confirmed the average sizes as ~30 nm for ZnO particles and ~ 70 nm for Ag doped ZnO particles. They are almost spherical and hexagonal wurtzite crystal structure. The experimental results indicated the enhanced photocatalytic ability of nanoZnO when doped with Ag. A maximum degradation of 98 % has been achieved in the total organic carbon of the carbaryl test solution of 5 ppm. It confirms the remarkable photocatalytic degradation activity of the synthesized Ag doped nanoZnO particles. The remarkable recycling ability of the synthesized nanoparticles ensured the purity of the catalyst as well. The present study confirmed that photodegradation capacity of nanoZnO under UV irradiation has increased after doping with Ag and it is an efficient and cost-effective method for the quick treatment of wastewater and other organic pollutants in water.

References

1. D. Gola, A. Kriti, N. Bhatt, M. Bajpai, A. Singh, A. Arya, N. Chauhan, S. K. Srivatsava, P. K. Tyagi, and Y. Agarwal, Curr. Res. Green Sustainable Chem. **4**, ID 100132 (2021). https://doi.org/10.1016/j.crgsc.2021.100132
2. J. Fenik, M. Tankiewicz, and M. Biziuk, Trends Anal. Chem. **30**, 814 (2011). https://doi.org/10.1016/j.trac.2011.02.008
3. S. Mostafalou and M. Abdollahi, Toxicol. Appl. Pharmacol. **268**, 157 (2013). https://doi.org/10.1016/j.taap.2013.01.025
4. D. B. Barr and L. L. Needham, J. Chromatography B **778**, 5 (2002). https://doi.org/10.1016/S1570-0232(02)00035-1
5. D. J. Ecobichon, Carbamate Insecticides, in: Handbook of Pesticide Toxicology, ed. R. Krieger (Academic Press, San Diego, 2001).https://doi.org/10.1016/B978-012426260-7/50055-0
6. S. Ampolu, S. P. Dalai, M. V. V. Ramanjaneyulu, U. Hanumantu, and A. Kumar, Biol. Forum – An Int. J.**15**, 2(2023).
7. M. Eddleston, Medicine **48**, 214 (2020). https://doi.org/10.1016/j.mpmed.2019.12.019
8. Z. Q. Jia, Y. C. Zhang, Q. T. Huang, A. K. Jones, Z. J. Han, and C. Q. Zhao, J. Hazard. Mater. **394**, ID 122521 (2020). https://doi.org/10.1016/j.jhazmat.2020.122521 122521
9. M. Sittig, Handbook of Toxic and Hazardous Chemicals and Carcinogens. 2nd Edition (Noyes Publications, Newzeland, 1985).
10. U. S. Environmental Protection Agency, Health and Environmental Effects Profile for Carbaryl. EPA/600/x84/155, Environmental Criteria and Assessment Office, Office of Health and Environmental Assessment, Office of Research and Development, Cincinnati, OH (1984).
11. The Merck Index,An Encyclopedia of Chemicals, Drugs, and Biologicals. 11 Edition, ed. S. Budavari (Merck and Co. Inc., Newzeland, 1989).
12. U. S. Department of Health and Human Services. Hazardous Substances Data Bank (HSDB, online database), National Toxicology Information Program, National Library of Medicine, Bethesda, MD. (1993).
13. U. S. Department of Health and Human Services. Registry of Toxic Effects of Chemical Substances (RTECS, online database), National Toxicology Information Program, National Library of Medicine, Bethesda, MD (1993).
14. U. S. Environmental Protection Agency. Integrated Risk Information System (IRIS) on Carbaryl, National Center for Environmental Assessment, Office of Research and Development (Washington, DC. 1999).

15. M. H. Pereza, G. Penuela, M. I. Maldonado, O. Malato, P. F. Ibanez, I. Oller, W. Gernjak, and S. Malato, Appl. Catal. B Environ. **64**, 272 (2006). https://doi.org/10.1016/j.apcatb.2005.11.013
16. S. G. Muhamad, Arab J. Chem. **3**, 127 (2010). https://doi.org/10.1016/j.arabjc.2010.02.009
17. M. Abdennouri, A. Galadi, N. Barka, M. Baalala, K. Nohair, M. Elkrati, M. Sadiq, and M. Bensitel, Phys. Chem. News **54** (2010).
18. N. Barka, S. Qourzal, A. Assabbane, A. Nounah, and Y. AitIchou, Arab J. Chem. **3**, 279 (2010). https://doi.org/10.1016/j.arabjc.2010.06.016
19. A. Satheesh, H. Usha, M. Visalakshi, T. Rambabu, Ch. V. V. Srinivas, Y. V. Kumar, and S. P. Douglas, Int. J. Eng., Res. Technol.**6**, 5 (2017). https://doi.org/10.17577/IJERTV6IS050467
20. D. Li, J. Wang, X. Wu, C. Feng, and X. Li, Ultrasonics Sonochem. **20**, 133 (2013). https://doi.org/10.1016/j.ultsonch.2012.05.017
21. S. Sibmah, E. K. Kirupavasam, Indian J. Chem. **61**, 901 (2022).
22. A. Nirmala and A. Anukaliani, Mater. Lett. **65**, 2645 (2011). https://doi.org/10.1016/j.matlet.2011.06.029
23. A. Satheesh and H. Usha, Int. J. Res. Culture Soc. **3**, 11(2019).
24. M. Ahmad, J. Zhao, J. Iqbal, W. Miao, L. Xie, R. Mo, and J. Zhu, J. Phys. D: Appl. Phys. 42, ID 165406 (2009).https://doi.org/10.1088/0022-3727/42/16/165406
25. A. Satheesh and H.Usha, Chem. Sci. Rev. Lett.**8**, 166 (2019).
26. T. Deepika, S. Anshu, S. R. Dharmender,T. Nagesh, S. Dilbag, T. Tomas, A. Mindaugas, T. Sigitas, K. S. Sudheesh, and T. Sourbh, Chemosensor **8**, 108 (2020). https://doi.org/10.3390/chemosensors8040108.
27. S. Iqbal, A. Bahadur, M. Javed, O. Hakami, R. M. Irfan, Z. Ahmad, and A. AlObaid, Mater. Sci. Eng.: B **272**, ID 115320 (2021). https://doi.org/10.1016/j.mseb.2021.115320
28. A. Irshad, A. Ejaz, and A. Mukhtar, SN Appl. Sci. **1**, ID 327 (2019). https://doi.org/10.1007/s42452-019-0331-9
29. A. Satheesh and H. Usha, Int. J. Res. Appl. Sci. Eng. Technol. **7**, 9 (2019).
30. S. Suresh,P. Kaushik, Z. C. Zaman, and M. H. Enamul, J. Sol-Gel Sci. Technol. **83**, 394 (2017). https://doi.org/10.1007/s10971-017-4418-8
31. S. Ampolu, D. Adinarayana, M. V. V. Ramanjaneyulu, H. Usha, Amitkumar, and K. N. Jogayya, J. Sci. Res. **16**, 311 (2024). https://doi.org/10.3329/jsr.v16i1.67363
32. M. Sudheere, G. Ravinder, G. Ravi, P. Venkataswamy, K. Vaishnavi, N. Chittibabu, and M. Vithal, Indian J. Chem. **59A**, 1092 (2020). https://doi.org/10.56042/ijca.v59i8.30553
33. D. K. Bhole, R.G. Puri, P. D. Meshram, and R. S. Sirsam, J. Indian Chem. Soc. **97**, 440 (2020).
34. R. R. Mathiarasu, A. Manikandan, K. Panneerselvam, M. George, K. K. Raja, M. A. Almessiere, Y. Slimani, A. Baykal, A. Ansari, T. Kamal, and A. Khan, J. Mater. Res. Technol. **15**, 5936 (2021). https://doi.org/10.1016/j.jmrt.2021.11.047
35. S. A. A. Anaam, H. Saim, M. Z. Sahdan, and A. Al-Gheethi, Int. J. Nanoelectron. Mater. **12**, 495 (2019).
36. S. Ampolu, U. Hanumanthu, D. S. Priya, A. V. L. N. H. Hariharan, M. V. V. Ramanjaneyulu, J. Sci. Res. **15**, 481 (2023).https://doi.org/10.3329/jsr.v15i2.60649
37. S. Ampolu, U. Hanumanthu, M. V. V. Ramanjaneyulu, K. N. Jogayya, A. Kumar, and S. P. Dalai, Mapana J. Sci. **22**, 97 (2023).
38. D. S. Priya, S. Ampolu, U. Hanumanthu, A. Hariharan, Chem. Sci. Rev. Lett. **11**, 356 (2022). https://doi.org/10.37273/chesci.cs205210390
39. S. Vasamsetty, S. Medidi, S. Ampolu, R. Majji, M. Kotupalli, C. C. Satyanarayana, A. Nowduri, and P. D. Sanasi, Green Sustainable Chem. **7**, 141 (2017). https://doi.org/10.4236/gsc.2017.72011.
40. Ch. Komali, N. Murali, K. Rajkumar, A. Ramakrishna, S. Y. Mulushoa, D. Parajuli, P. N. V. V. L. P. Rani, S. Ampolu, K. C. Mouli, and Y. Ramakrishna, Chem. Papers **77**, 109 (2022). https://doi.org/10.1007/s11696-022-02466-9.